

Development of electrically conductive microstructures based on polymer/CNT nanocomposites via two-photon polymerization

U. Staudinger^{1*}, G. Zyla², B. Krause¹, A. Janke¹, D. Fischer², C. Esen², B. Voit¹, A. Ostendorf²

¹ Leibniz Institute of Polymer Research Dresden (IPF), Hohe Str. 6, 01069 Dresden, Germany

² Ruhr-University Bochum, Applied Laser Technologies, Universitätsstr. 150, 44780 Bochum, Germany

Abstract

Femtosecond laser-induced two-photon polymerization (2PP) of carbon nanofiller doped polymers was utilized to produce electrically conductive microstructures, which are expected to be applicable as microelectronic components or micro-electromechanical systems in sensors. The nanocomposites were processed by compounding an inorganic-organic hybrid material with two different types (short and long) of single walled carbon nanotubes (SWCNTs). Different SWCNT contents were dispersed in the polymer by sonication to adjust the electrical conductivity of the nanocomposites. Low surface resistivity values of $\sim 4.6 \times 10^5 \Omega/\text{sq.}$ could be measured for coated reference films with a thickness of 30 μm having an exceptionally low SWCNT content of 0.01 wt% of the long type of SWCNTs. In contrast, a higher minimum resistivity of $1.5 \times 10^6 \Omega/\text{sq.}$ was exhibited for composites with a higher content, 2 wt%, of short SWCNTs. The structural quality of the microstructures processed by 2PP was mainly influenced by the dispersion quality of the SWCNTs. To characterize the electrical conductivity, conductive atomic force microscopy was applied for the first time. In microstructures with 0.05 wt% of the long type of SWCNTs, a contact current could be detected over a wide range of the

* Corresponding author. Tel: 0049 351 4658 646. E-mail: staudinger@ipfdd.de (Ulrike Staudinger)

measured area visualizing the electrical conductive CNT network, which has not been reported before.

Keywords: conductive nanocomposite, carbon nanotube, two-photon polymerization, microstructure

1 Introduction

Two-photon polymerization (2PP) is a novel laser microfabrication method to generate complex three-dimensional microstructures with submicron resolution using a femtosecond laser [1-6]. In addition to purely organic acrylate- or epoxy-based polymers [3, 7-9] multifunctional inorganic-organic hybrid polymers (e. g. Ormocers from Micro Resist Technology GmbH) can be used for the microfabrication process; these materials are synthesized by sol-gel processing, and combine the properties of organic polymers with those of glasslike materials [10-12]. For practical application as microelectronic components or micro-electromechanical systems (MEMS), enhancement of the optical, magnetic or electrical properties of a polymer is often required. For example, coloured microstructures have been realized by doping the polymer with CdS nanoparticles [13]. Other examples are the modification of the refractive index by adding TiO₂ nanoparticles [14,15] or the usage of Fe₃O₄ nanoparticles for electromagnetic applications [16-18].

To fabricate electrically conductive microstructures via 2PP, single walled carbon nanotubes (SWCNTs) were added to different polymer, where in one case the bulk composite material containing 2 wt% to 5 wt% of SWCNTs has been proved to reach an electrical conductivity of maximum 1.3×10^{-7} S/m [19]. In another case, SWCNTs have been found to be aligned along the fabricated nanowire axis, indicating the formation of a CNT network [20]. Otuka et al. fabricated microstructures with good surface quality

using SWCNTs functionalized with carboxylic acid [21]. However, no sufficient information about the electrical conductivity of the fabricated microstructures has been available so far.

When using absorbing nanofillers like CNTs, the dispersion of the nanofillers within the polymer has to take place very homogeneously to avoid local absorption peaks during laser writing. A high local concentration of nanotubes hinders the transmission of the laser leading to an interruption of the writing process, which causes defects in the microstructure. A sufficient distribution and dispersion of the CNTs within the polymer can be reached by applying sonication, a process which generates cavitation to break the CNT agglomerates. The parameters of sonication including duration, frequency and amplitude have to be adjusted according to the used matrix polymer, CNT type and CNT concentration. As the dispersion quality deteriorates with increasing CNT concentration, the amounts of CNTs to be added to the polymer matrix are limited. In principle, very low percolation thresholds ranging between 0.0021 wt% and 0.024 wt%, have been reached in polymer/CNT composites [22-25]. It was demonstrated, that the percolation threshold depends on the nanotube length and on composite processing conditions such as stirring rate and temperature [24, 25].

~~Hence the formation of a polymer/CNT composite system that incorporates a highly conductive SWCNT type is very suitable for the 2PP process to fabricate high quality conductive microstructures.~~

This paper presents the development of electrically conductive polymer/SWCNT composites and their microstructuring via 2PP. Two types of SWCNTs were selected as nanofiller due to their good dispersability and electrical performance based on previous experience and studies [19, 30]. The electrical conductivity of the microstructures was

investigated applying conductive atomic force microscopy (C-AFM). Due to its high spatial resolution, this method is very suitable to study the local electrical properties of small scale structures [26].

2 Experimental

2.1 Materials

The photosensitive inorganic-organic hybrid material Femtobond 4B (Laserzentrum Hannover e.V., Germany), herein after referred to as Femtobond, was used as matrix polymer. As a conductive filler, both single walled carbon nanotubes (SWCNTs) from OCSiAl (Tuball) with a length $> 5 \mu\text{m}$ and a diameter of 1.6 nm [27] and SWCNTs from Nanostructured & amorphous Materials Inc. (Nanoamor) with a length of 1-3 μm and an average outside diameter of 1.1 nm [28] were used. According to the manufacturer, neither CNT type is functionalized. The powder conductivity of the SWCNTs was characterized based on the assumption that the electrical conductivity of the nanotubes itself may influence the electrical properties of the composite. The measurement was carried out under pressure using a homemade measuring cell combined with an analysis software based on Agilent VEE Version 9.3 as described and applied elsewhere [29]. At a pressure of 30 MPa the powder conductivity results of both SWCNT types were determined to be comparable exhibiting mean values of 36.4 S/cm for Tuball and 34.3 S/cm for Nanoamor with bulk densities of 0.32 and 0.34 g/cm^3 , respectively. By comparison, MWCNTs exhibit powder conductivity values in the range of 4 and 30 S/cm [Ameli A, Arjmand M, Pötschke P, Krause B, and Sundararaj U. Carbon 2016;106:260-278.;

Krause B, Boldt R, Häußler L, and Pötschke P. *Composites Science and Technology* 2015;114:119-125;

Arjmand M, Chizari K, Krause B, Pötschke P, and Sundararaj U. *Carbon* 2016;98:358-372;

Krause B, Pötschke P, Ilin E, and Predtechenskiy M. *Polymer* 2016;98:45-50.].

2.2 Preparation of polymer/SWCNT dispersion

Various contents of SWCNTs were each dispersed in 10 ml Femtobond and sonicated for certain times using an ultrasonic processor (UP400S, Hielscher) with a sonotrode of type H3. Based on our previous experience and studies, the SWCNT concentration and the sonication time were selected as shown in Table 1. Femtobond/SWCNT dispersions with Nanoamor were prepared with SWCNT concentrations of 1 wt% and 2 wt% and sonicated for 30 min. These parameters were selected according to prior related studies of Guo et al. [19]. Parameter selection for dispersions with Tuball SWCNTs was based on other studies using Tuball in thermoplastics such as polypropylene [30]. First a Tuball concentration of 1 wt% was selected. After only a few minutes of sonication the viscosity of the dispersion increased significantly to the point that the treatment had to be aborted. Therefore, the Tuball concentration was decreased to 0.1 wt% in the following experiment. Due to the good dispersability of the Tuball SWCNTs and the low electrical resistivity values of the prepared composite films, which will be discussed in this paper, low sonication time of 10 min and further low SWCNT concentrations of 0.05 wt% and 0.01 wt% were selected for the preparation of the Femtobond/SWCNT dispersions.

Table 1 Preparation of Femtobond/SWCNT dispersions

SWCNT type	SWCNT length(μm)	SWCNT content (wt%)	Sonication time (min)
Nanoamor	1-3 [28]	1 and 2	30
Tuball	> 5 [27, 30]	0.05	10 and 20
		0.1 and 0.01	10

2.3 Processing of polymer/SWCNT composite films

After sonication, films of 30 μm and 60 μm were prepared by coating the dispersion on a polyimide sheet using a Quadruple Film Applicator, Model 360 from Erichsen, Germany. Additionally the dispersions were coated on glass slides by dropwise addition of 100 μl . The films were dried on a heating plate for one hour using a temperature interval from 60 $^{\circ}\text{C}$ to 100 $^{\circ}\text{C}$ as suggested for Femtobond by the supplier. The polymerization of the Femtobond material was conducted applying UV light with a wavelength of 365 nm for 48 hours.

2.4 Characterization of SWCNT dispersion in nanocomposite films

To characterize the dispersion of SWCNTs in the composite films transmission light microscopy (TLM) was performed using a Leica an Olympus-BH2 microscope combined with a camera DP71 (Olympus Deutschland GmbH, Germany).

2.5 Electrical resistivity measurements

The surface resistivity was measured on the coated composite films using a Loresta electrometer from Mitsubishi with a measuring range between $10^{-3} \Omega$ and $10^7 \Omega$ for samples with resistances $< 10^7 \Omega$. Hiresta electrometer from Mitsubishi with a measuring range between $10^4 \Omega$ and $10^{13} \Omega$ was used for samples with resistances $> 10^7 \Omega$. The

Loresta was used with a 4-point electrode (ESP) with an electrode distance of 5 mm and an electrode diameter of 2 mm. The Hiresta was connected to a ring electrode (URS) with the inner electrode having a diameter of 5.9 mm and the exterior electrode having an inner and outer diameter of 11 mm and 18 mm respectively. On each film five measurements were conducted and the arithmetical average and the standard deviation were calculated. In order to differentiate the surface resistivity from the surface resistance it is expressed in Ohm/square ($\Omega/\text{sq.}$).

2.6 Fabrication of microstructures via two-photon polymerization

An ultrafast Ti:sapphire laser (Tsunami, Spectra Physics) with a pulse duration of 90 fs, a repetition rate of 82 MHz and a wavelength of 780 nm and an output beam diameter < 2 mm was used for the fabrication of conductive microstructures via 2PP with a single pulse energy density between $0.8 \text{ nJ}/\mu\text{m}^2$ and $1 \text{ nJ}/\mu\text{m}^2$ in the focus area. A drop shaped volume of the polymer/SWCNT dispersion was given on a coverslip and was placed on a spacer with the polymer on the bottom side as shown in Fig. 1a. The average laser power was measured by a photodiode and could be adjusted by a combination of a motorized rotatable $\lambda/2$ -plate and a polarization beam splitter cube. Due to the high photon density which is required for the initiation of the polymerization of the polymer, a strong focussing oil-immersion microscope objective with a 100 x magnification and a numeric aperture of 1.4 had to be used. The polymerization threshold of Femtobond 4B could be investigated for single pulse density of approximately $0.15 \text{ nJ}/\mu\text{m}^2$. Arbitrary layers can be fabricated with an acousto-optic modulator (AOM) as a fast shutter, and the deflection of the laser beam with a galvo-scanner (hurryScan II, Scanlab). The rise and fall time of the AOM (MCQ110-A2.5-IR, AA Optoelectronic) is defined with 115 ns/mm. The maximum scan speed of the galvo scanner is 1.5 m/s. After each layer, the height of the

sample is shifted by a mechanical stage (Wafer Z, Aerotech) to get 3D structure geometry. The maximum velocity of the mechanical stage is 4 mm/s. The laser beam is focussed through a transparent coverslip into a drop-shaped volume of the resin-SWCNT dispersion as shown in the image section of Fig. 1a. The coverslip function as an adhesive material for the resin. But simultaneously it is important to ensure tightly focussing with immersion oil. With the usage of planar self-traveling stage (ANT 130-110-XY, Aerotech) several individual microstructures could be generated on one single substrate. After exposure, the polymer/SWCNT dispersion was developed in 1-propanol for 30 min followed by an air-drying to evaporate the developer solution. Unexposed polymer was dissolved in the chemical solution, while the exposed areas adhered to the coverslip.

For the electrical characterization of the microstructures via C-AFM as described below, a conductive base substrate material was required, which works as an anode in the measurement process. Thus, a gold layer with a thickness of 20 nm was sputtered (model k575x, Emitech) for 180 s with a current of 60 mA on the top of a glass substrate. During the sputtering process the vacuum level was 10^{-4} mbar. In the next step a gold coating was tested due to successful proved applicability as a base substrate material for UV lithography [31]. Due to the high reflectivity of gold in the NIR range, the laser beam is incapable of penetrating a gold coated coverslip and to polymerize the polymer-SWCNT. Thus the 2PP set-up had to be extended. An adaptor consisting of two cylindrical aluminium components was used as shown in Fig. 1b, as demonstrated by Obata et al. [32]. The internal and external adaptor can be screwed together. At the lower end of the internal adaptor a thin coverslip was fixed with a glue to protect the microscope and to enable the usage of immersion oil to focus the laser beam correctly. With this configuration a drop shaped volume of polymer-SWCNT dispersion can be put directly

on top of the base material's coated upper side. By focusing the laser beam through the photosensitive material the polymerization starts at the gold coated surface.

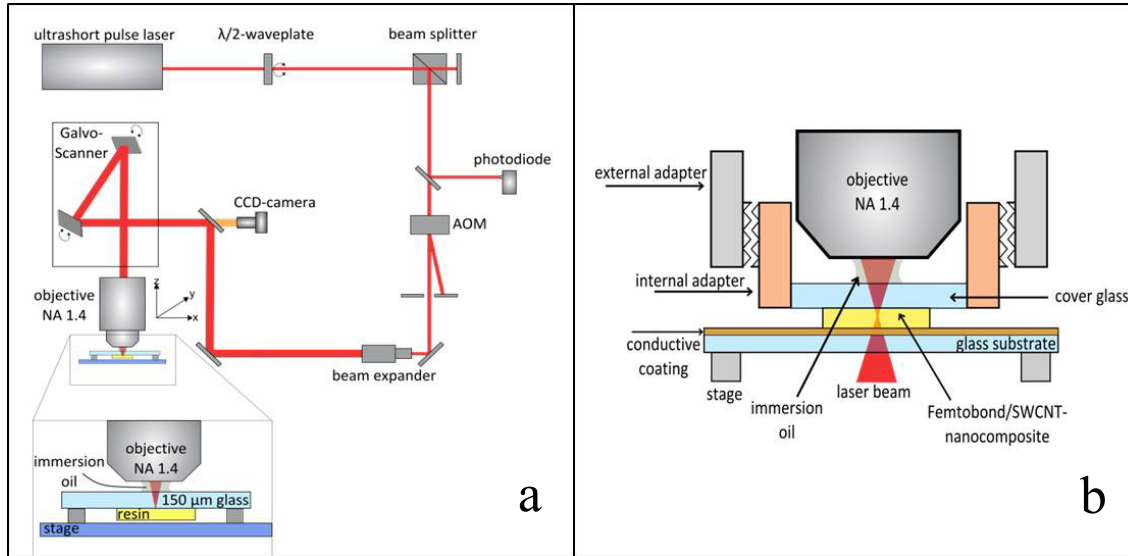


Figure 1 Experimental set-up for the fabrication of microstructures with a two-photon polymerization process (a). Extension of the 2PP set-up (b) to increase the work distance of the objective and to enable the fabrication of microstructures on different substrates. Two adapters can be screwed together to protect the microscope objective and to ensure precise focusing of the laser beam into the material.

2.7 Characterization of the structural quality of the microstructures

For the structural characterization of the microstructures, a scanning electron microscope (SEM) EVO MA 15 from Zeiss, Germany was used. Therefore, the samples were sputtered with a combined target of gold and palladium for 120 s using a current of 20 mA. For a rough evaluation of the structural quality overview pictures of the microstructures were additionally generated using a light microscope Eclipse LV 100 (Nikon, Japan).

2.8 Conductive - atomic force microscopy measurements

To characterize the electrical conductivity of the microstructures, conductive atomic force microscopy (C-AFM) measurements were done in contact mode using a Dimension ICON (Bruker-Nano, USA) equipped with a Peak Force TUNA application module for measurement of the contact current. Cr/Pt coated silicon-SPM-sensors Multi75E (BudgetSensors, Bulgaria) with spring constant of ca. 4 N/m and with a tip radius lower than 25 nm were used. The microstructures to be measured were prepared on glass substrates coated with a gold layer. The samples were contacted by silver paste and a voltage V of 100 mV was applied between sample and tip. The generated current I during the scan and the topographic information (height images) were detected.

3 Results

3.1 SWCNT dispersion and network formation

The two types of SWCNTs used in this study significantly differ in their lengths and their dispersability in the Femtobond polymer, influencing their ability to form a percolating network. TLM images in Fig. 2 represent the SWCNT dispersion in a Femtobond/SWCNT composite with 0.1 wt% of the long Tuball-SWCNTs (Fig. 2a) and in a composite with 1 wt% of the short Nanoamor-SWCNTs (Fig. 2b), both prepared on glass slides. Tuball-SWCNTs were distributed and dispersed very homogeneously in the Femtobond matrix. Partially very long bundles of SWCNTs with a length to about 100 μm are visible. In contrast, Nanoamor-SWCNTs were more agglomerated and formed a cloud-like network within the polymer matrix.

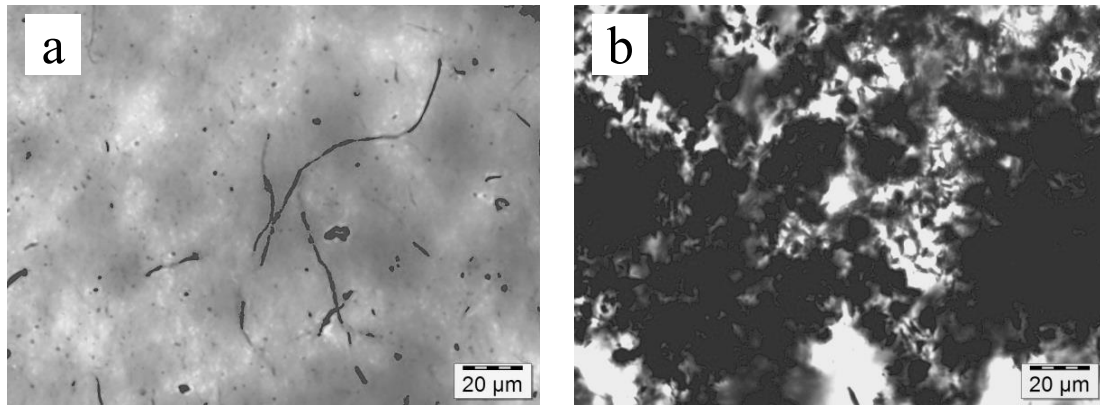


Figure 2 TLM images of Femtobond/SWCNT composite films with 0.1 wt% Tuball (a) and with 1 wt% Nanoamor (b), both prepared on glass slides

Fig. 3 shows the TLM images of selected Femtobond/SWCNT composites with a thickness of 30 μm coated on polyimide sheets. As shown in Fig. 3a, composites with only 0.05 wt% Tuball (sonication of 20 min) already formed a very good SWCNT network. The impact of such SWCNT percolation on the electrical properties is clearly reflected in the low surface resistivity of about $1.1 \times 10^5 \Omega/\text{sq.}$, as displayed in Fig. 4.

Decreasing the sonication time to 10 min while keeping the Tuball content constant has no significant effect on the surface resistivity of the composite. Increasing the Tuball content to 0.1 wt% only causes a slight decrease of the resistivity, which however remains within the range of error in the measurement. When the Tuball concentration is decreased to 0.01 wt% the surface resistivity increases to about $4.6 \times 10^5 \Omega/\text{sq.}$, which is still exceptionally low considering the very small amount of added SWCNTs. Another study of epoxy-amine /MWCNT composites revealed an electrical percolation threshold at MWCNT contents between 0.019 wt% and 0.037 wt%, using MWCNTs Baytube 150P (purity > 95 %, average diameter 13-16 nm, length >1 μm) [33].

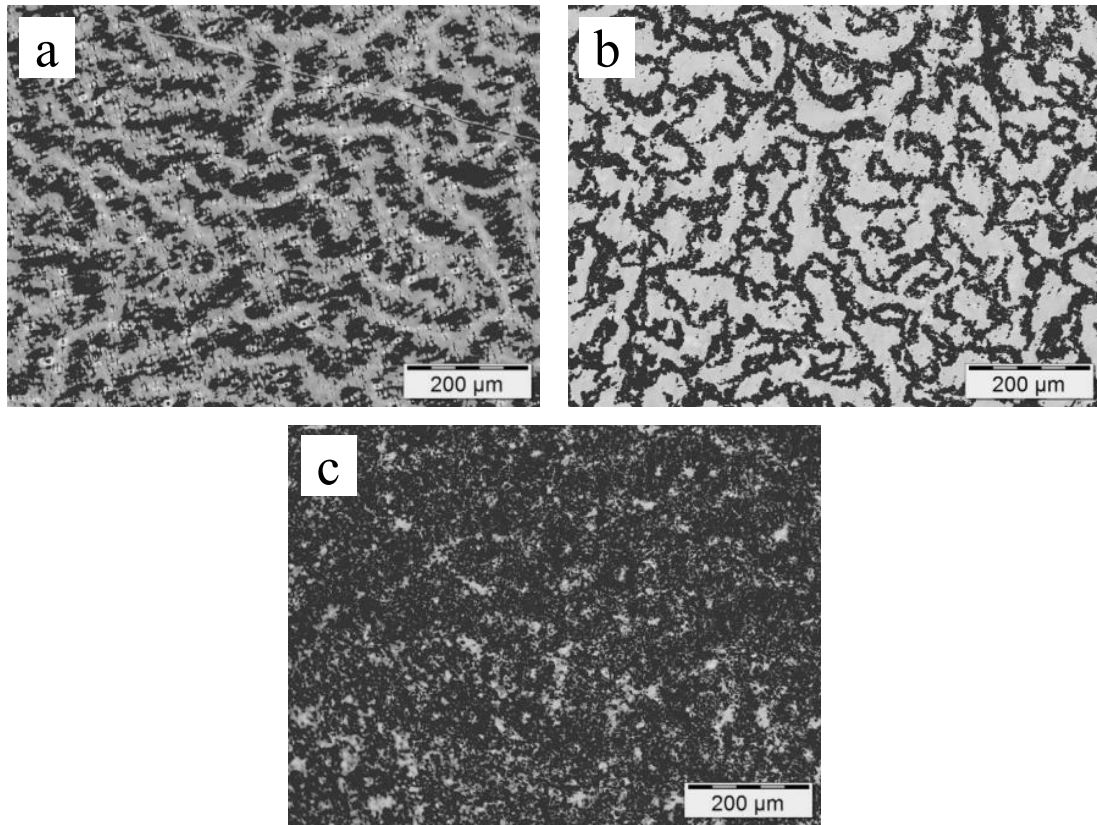


Figure 3 TLM images of Femtobond/SWCNT composite films with 0.05 wt% Tuball, 20 min sonication (a) with 1 wt% Nanoamor (b) and with 2 wt% Nanoamor (c); prepared on polyimide sheets with a thickness of 30 μm

Fig. 3b shows the formation of a SWCNT network within a composite containing 1 wt% of Nanoamor. However, the surface resistivity of $3.2 \times 10^7 \Omega/\text{sq.}$ exceeds the value of the composite with 0.01 wt% Tuball-SWCNTs by about two orders of magnitude despite containing a 100 times larger weight content of SWCNTs (Fig. 4). It must be noted that Tuball-SWCNTs are particularly long, enabling the CNT network formation at much lower SWCNT content than in composites containing the shorter Nanoamor-SWCNTs. The favorable effect of the high nanotube aspect ratio of Tuball-SWCNTs combined with a good state of macrodispersion on the electrical percolation was found recently studying polypropylene based composites [30].

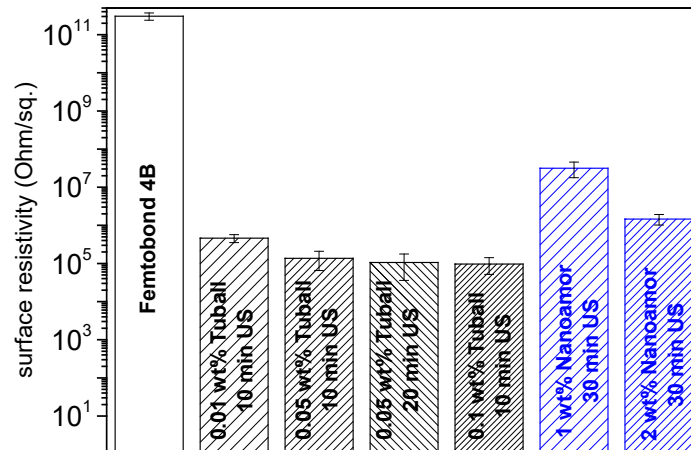


Figure 4 Surface resistivity of Femtobond/SWCNT composite films prepared on polyimide sheets with a thickness of 30 μm ; US: ultra sonication treatment

To improve the electrical conductivity of the Femtobond/Nanoamor composites the addition of Nanoamor-SWCNTs was increased to 2 wt%. The TLM image in Fig. 3c shows a very dense SWCNT network. The surface resistivity decreased to about 1.5×10^6 Ω/sq . (Fig. 4) which is still larger than for the Femtobond/0.01 wt% Tuball composite.

The surface resistivity was also measured on coated composite films with a thickness of 60 μm . The results were comparable to the values of films with a thickness of 30 μm and are not shown here.

3.2 Microstructuring of SWCNT dispersions

For the microstructuring process via 2PP it is important to ensure a very homogeneous dispersion of the absorbing SWCNTs in the Femtobond polymer to avoid local absorption peaks. High local SWCNT concentrations inhibit the transmission of the laser beam and therefore disrupt the fabrication process (i.e. damage of the microstructure).

Structuring of the Femtobond/SWCNT dispersions was first performed at uncoated glass substrates using dispersions with 1 wt% and 2 wt% Nanoamor and with 0.05 wt% and

0.1 wt% Tuball. For the structuring process, a large average power (P) between 30 mW and 50 mW had to be used due to the high absorption of the SWCNTs. However, to reach complete polymerization, the scanning speed (v) had to be kept low and was set between 50 $\mu\text{m/s}$ and 300 $\mu\text{m/s}$. In contrast, to polymerize the matrix polymer Femtobond without any SWCNT doping, the average power could be adjusted in a lower range between 12 mW and 25 mW and distinct higher scanning speed of 500 $\mu\text{m/s}$ to 2000 $\mu\text{m/s}$ could be used.

In Fig. 5, SEM images of valve structures, processed from dispersions with 1 wt% Nanoamor (Fig. 5a) and 0.1 wt% Tuball (Fig. 5b) and from pure Femtobond (Fig. 5c) are shown. For comparison, a computer-aided design (CAD) drawing of the valve is shown in Fig. 5 d. Generally, it was found that microstructures generated from Femtobond/Tuball dispersions show a distinct higher quality than microstructures produced from the higher SWCNT-concentration Femtobond/Nanoamor dispersions. The latter exhibit a large number of defects, caused by remaining CNT agglomerates in the dispersion, as visible in Fig. 5a. In Femtobond/Tuball microstructures the surfaces exhibit higher structural integrity. However, the long Tuball-SWCNTs protruding the microstructure and connecting with the substrate can be clearly identified (Fig 5b). In comparison, microstructures processed from pure Femtobond exhibit a very good surface quality and structural integrity (Fig 5c).

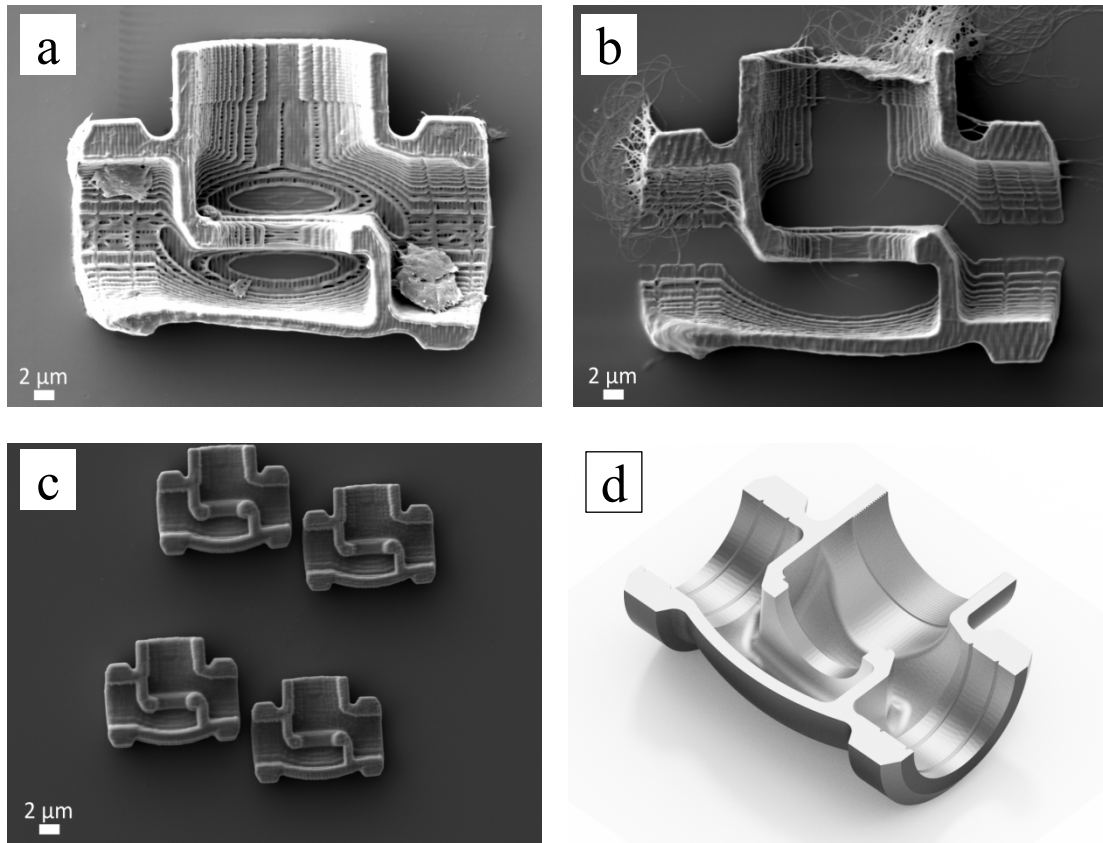


Figure 5 Microstructures of valves fabricated from Femtobond/SWCNT dispersions with 1 wt% Nanoamor at an average laser power $P = 32$ mW and a scanning speed $v = 100$ $\mu\text{m/s}$ (a), dispersions with 0.1 wt% Tuball at $P = 32$ mW and $v = 100$ $\mu\text{m/s}$ (b) and from pure Femtobond at $P = 25$ mW and $v = 1.7$ mm/s (c); computer-aided design (CAD) model of the valve (d)

The quality of the microstructures depends on the resolution, i.e. the linewidth. In Fig. 6a and b 3D grid structures (wood piles) generated from a dispersion containing 0.05 wt% Tuball SWCNTs and sonicated for 10 min, are presented. The minimum measured linewidth is about 450 nm. Single SWCNTs and bundles of SWCNTs protrude or superimpose the structure, which could turn out to be unsuitable for the production of high quality microstructures. Comparing the SEM images of these microstructures with those of a Femtobond/SWCNT composite containing the same amount of Tuball-SWCNTs but treated with 20 min of sonication (Fig. 6c and d), a quality-difference of the microstructures could be detected. The increase in sonication time results in an

improved dispersion of the SWCNTs in the Femtobond polymer and might be combined with shortening of SWCNTs caused by the ultrasonic vibration. Thus the microstructures are predominantly free from defects and exhibit significantly less remaining SWCNT bundles or agglomerates.

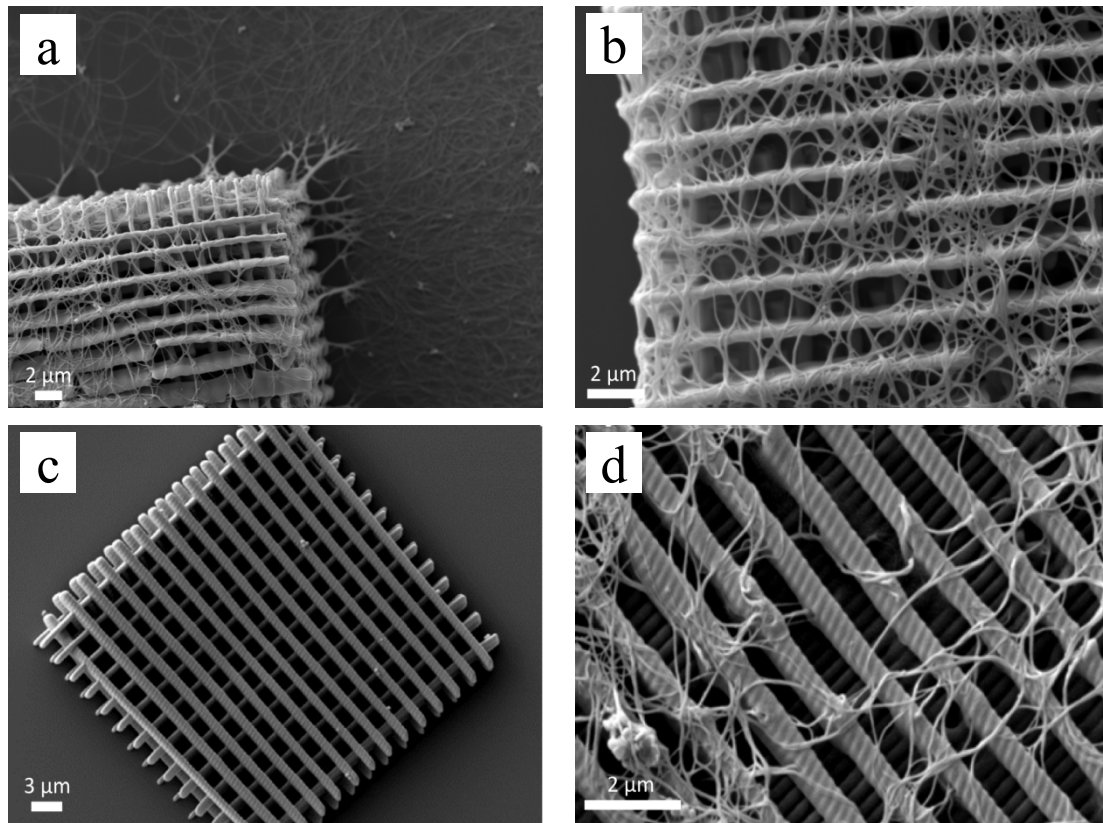


Figure 6 3D microstructures of a grid (woodpile) fabricated from Femtobond/SWCNT dispersions with 0.05 wt% Tuball sonicated for 10 min, $P = 30$ mW, $v = 50$ $\mu\text{m/s}$ (a, b) and dispersions with 0.05 wt% Tuball sonicated for 20 min, $P = 25$ mW, $v = 8$ $\mu\text{m/s}$ (c, d).

3.3 Conductive behavior of microstructures

Information about the local electrical conductance of the microstructures could be obtained using C-AFM by visualizing the charge transport from the lower electrode through the volume of the sample up to its surface.

To prepare microstructures for C-AFM measurements, Femtobond/SWCNT dispersions with 1 wt% and 2 wt% Nanoamor and dispersions with 0.01 wt% and 0.05 wt% Tuball (10 min US) were selected. The structuring process was carried out on glass substrates sputtered with a gold layer with a thickness of 20 nm. As the dispersion had to be deposited on the top of the substrate, the focus of the laser beam had to be transferred through the whole material. Thus light absorption caused by the SWCNT agglomerates is promoted, leading to a distinct power loss of the laser beam. Therefore the laser power had to be increased considerably to 80 mW.

Line structures of a Femtobond/0.01 wt% Tuball composite are predominantly free from defects (Fig.7a). However, several long SWCNTs are overlapping the structure. Line structures of a Femtobond/1 wt% Nanoamor composite contain a large number of SWCNT agglomerates, which negatively influence the quality of the microstructure (Fig 7b). During the performance of C-AFM measurements no contact current could be detected for either type of composites, implying that the microstructures were not electrically conductive. Additionally, the line structure geometry was found not to be suitable for the contact measurement as no continuous scan of the cantilever tip over the entire microstructure could be performed.

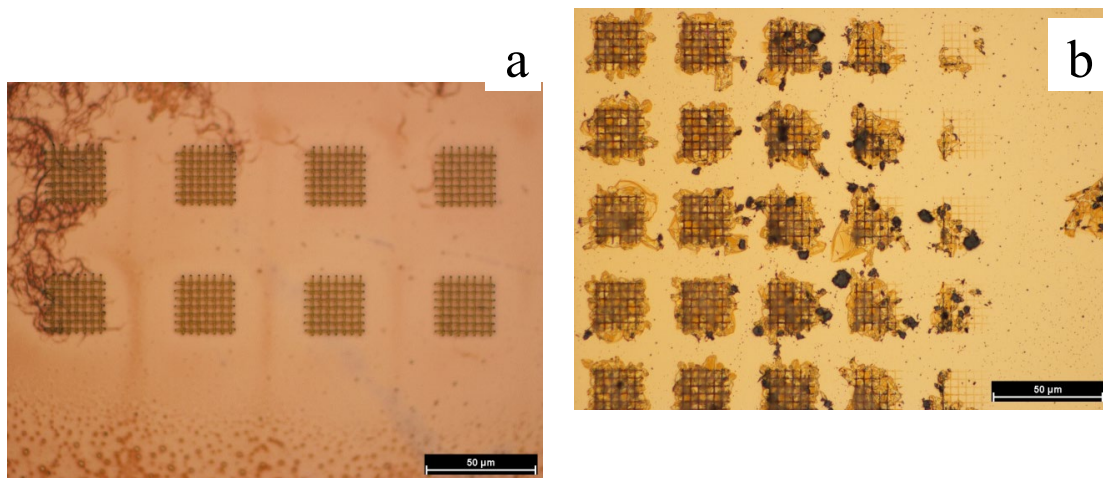


Figure 7 Light microscope images of planar grid structures of Femtobond/SWCNT dispersions with 0.01 wt% Tuball (a) and 1 wt% Nanoamor (b); $P = 25$ mW, $v = 1.7$ mm/s; scale bar 50 μm .

To investigate the electrical behavior of composite structures containing 0.05 wt% Tuball and 2 wt% Nanoamor microstructures in the shape of a cube were processed.

In Fig. 8 height and contact current images of Femtobond/2 wt% of Nanoamor composite are presented. The microstructures exhibit only confined small conductive areas with current values in the range of 50 to 550 nA, indicating that the SWCNT network is not homogeneously formed throughout the whole volume of the composite structure (Fig 8b).

In most cases, no contact current could be measured at the surface of the samples. In many cases SWCNT agglomerates cover the microstructures or are concentrated at their edges.

The tendency of Nanoamor-SWCNTs to form agglomerates hinders the laser structuring process and does negatively influence the electrical conductivity of the composites. From the topography measurement the thickness of the microstructures was found to be approximately 1 μm (Fig. 8a). In microstructures with 0.05 wt% of Tuball SWCNTs a contact current in the range of 20 to 400 nA could be detected (Fig. 9b). The SWCNT network is excellently formed throughout the volume of the matrix as visualized by the height image in Fig. 9a. However, this only applies to few samples, mainly unfolded structures having a thickness of only 150 to 200 nm. Other microstructures of Femtobond/Tuball composites do not exhibit any contact current signal due to the presence of SWCNT agglomerates and bundles hindering the formation of a defect-free microstructure.

Overall, Tuball-SWCNTs are very suitable as filler in dispersions used for 2PP, due to their good dispersability and the low percolation thresholds. However, their high length and the presence of SWCNT bundles are very challenging for the processing of high-quality microstructures. As described in section 3.2, the quality of the microstructures

was improved by increasing the sonication time of the Femtobond/Tuball dispersion. Additionally, the electrical resistivity of the bulk material remained on a low level (Fig. 4). Consequently, further studies will concentrate on the investigation of Femtobond/Tuball nanocomposites with very low SWCNT content but increased sonication treatment to decrease the amount of SWCNT bundles and to sufficiently shorten the SWCNTs to ensure the reproducible fabrication of defect-free and electrically conductive microstructures.

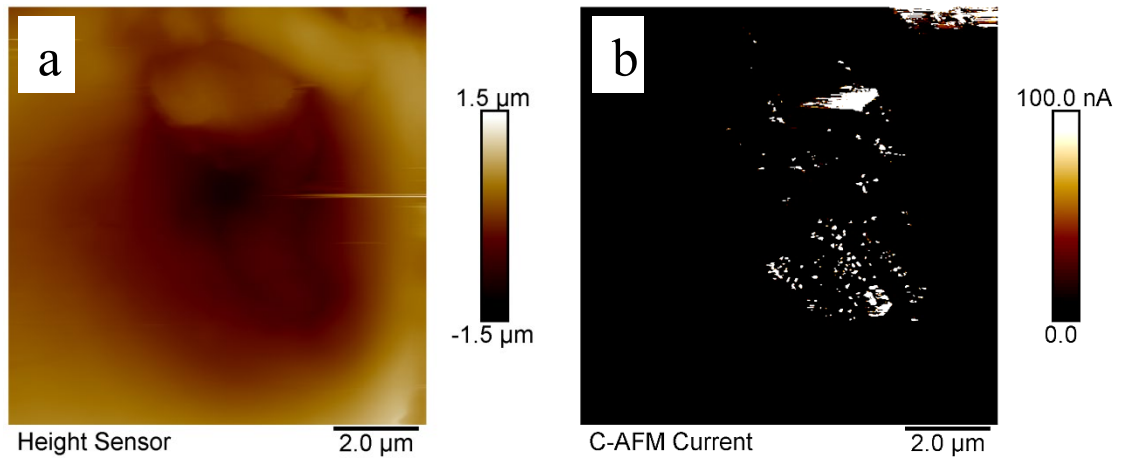


Figure 8 Topography (a) and contact current signals (b) of a microstructure with 2 wt% Nanoamor, C-AFM measurement, $V = 100 \text{ mV}$, $I = 50 \dots 550 \text{ nA}$.

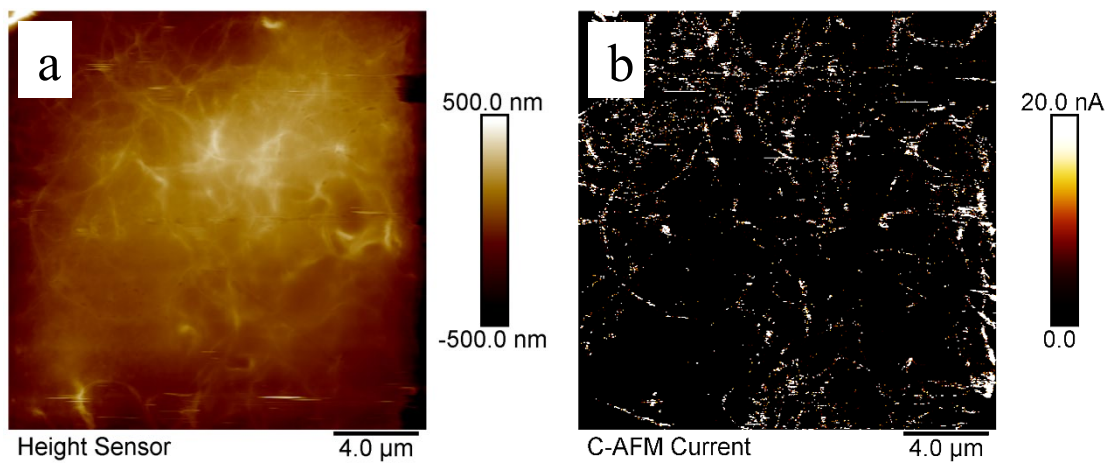


Figure 9 Topography (a) and contact current signals (b) of a microstructure with 0.05 wt% Tuball, C-AFM measurement, $V = 100$ mV, $I = 20 \dots 400$ nA.

4 Summary and conclusion

The present study demonstrates the viability of processing electrically conductive microstructures by laser-induced two-photon polymerization of polymer/SWCNT nanocomposites and their electrical characterization by the performance of C-AFM. Nanocomposites were produced by compounding the inorganic-organic hybrid material Femtobond 4B with two types of SWCNTs, which significantly differ in their length, i.e. their aspect ratio. Varying contents of SWCNTs were dispersed in the Femtobond polymer by sonication. The electrical surface resistivity of nanocomposite films, which were coated on polyimide sheets, was found to be highly dependent on the used SWCNT type. Nanocomposites containing the long type of Tuball SWCNTs exhibit low resistivity values of $4.6 \times 10^5 \Omega/\text{sq.}$ at an exceptionally low SWCNT amount of 0.01 wt%, implying a very low percolation threshold what, for polymer/CNT composites, has not been reported before. In contrast, for composites containing the short type of Nanoamor SWCNTs a significantly larger nanofiller content of 2 wt% was required to obtain a surface resistivity of $1.5 \times 10^6 \Omega/\text{sq.}$ The structural quality of the microstructures processed via 2PP was adjusted by optimizing the laser performance and the scan speed and was mainly influenced by the dispersion quality of the SWCNTs. Using the C-AFM method it was possible for the first time to characterize the electrical conductivity of the microstructures. The electrical conductive CNT network formed in microstructures with 0.05 wt% of Tuball SWCNTs could be visualized. However, other microstructures did not exhibit any contact current signal due to the presence of SWCNT agglomerates and bundles hindering the formation of a defect-free microstructure. By further optimization

of the SWCNT dispersion and development of a controlled and reproducible microstructuring process it is aimed to design composite microstructures to be applicable as microelectronic components or micro-electromechanical systems (MEMS) in sensors.

Acknowledgement

The authors thank the German Research Foundation (DFG) for financial support of this project (GZ: STA 1392/2-1, VO 583/29-1, ES 182/8-1).

References

- [1] S. Maruo, O. Nakamura, S. Kawata, Three-dimensional microfabrication with two-photon-absorbed photopolymerization, *Opt. Lett.* 22 (1997) 132-134.
- [2] S. Kawata, H.-B. Sun, T. Tanaka, K. Takada, Finer features for functional microdevices, *Nature* 412 (2001) 697-698.
- [3] H.-B. Sun, T. Kawakami, Y. Xu, J.-Y. Ye, S. Matsuo, H. Misawa, M. Miwa, R. Kaneko, Real three-dimensional microstructures fabricated by photopolymerization of resins through two-photon absorption, *Opt. Lett.* 25 (2000) 1110-1112.
- [4] A. Ostendorf, B. N. Chichkov, Two-Photon Polymerization: A New Approach to Micromachining, *Photonics Spectra* 40 (2006) 72-79.
- [5] M. Malinauskas, M. Farsari, A. Piskarskas, S. Juodkazis, Ultrafast laser nanostructuring of photopolymers: A decade of advances, *Phys. Rep.* 533 (2013) 1-31.
- [6] M. Farsari, B. Chichkov, Materials processing: Two-photon fabrication, *Nature Photonics* 3 (2009) 450-452.
- [7] T. Baldacchini, C. N. LaFratta, R. A. Farrer, M. C. Teich, B. E. A. Saleh, M. J. Naughton, J. T. Fourkas, Acrylic-based resin with favorable properties for three-dimensional two-photon polymerization, *J. Appl. Phys.* 95 (2004) 6073-6074.

- [8] R.J. Winfield, S. O'Brien, Two-photon polymerization of an epoxy–acrylate resin material system, *Appl. Surf. Sci.* 257 (2011) 5389-5392.
- [9] H.-B. Sun, K. Takada, S. Kawata, Elastic force analysis of functional polymer submicron oscillators, *Appl. Phys. Lett.* 79 (2001) 3173-3175.
- [10] J. Serbin, A. Egbert, A. Ostendorf, B. N. Chichkov, R. Houbertz, G. Domann, J. Schulz, C. Cronauer, L. Fröhlich and M. Popall, Femtosecond laser-induced two-photon polymerization of inorganic–organic hybrid materials for applications in photonics, *Opt. Lett.* 28 (2003) 301-303.
- [11] A. Greiner, B. Richter, M. Bastmeyer, Micro-Engineered 3D Scaffolds for Cell Culture Studies, *Macromol. Biosci.* 12 (2012) 1301-1314.
- [12] A. Ovsianikov, J. Viertl, B. Chichkov, M. Oubaha, B. MacCraith, I. Sakellari, A. Giakoumaki, D. Gray, M. Vamvakaki, M. Farsari, C. Fotakis, Ultra-Low Shrinkage Hybrid Photosensitive Material for Two-Photon Polymerization Microfabrication, *ACS Nano* 2 (11) (2008) 2257–2262.
- [13] Z. B. Sun, X. Z. Dong, W. Q. Chen, S. Nakanishi, X. M. Duan, S. Kawata, Multicolor polymer nanocomposites: In situ synthesis and fabrication of 3D microstructures, *Adv. Mater.* 20 (2008) 914-919.
- [14] Q. Guo, R. Ghadiri, S. Xiao, C. Esen, O. Medenbach, A. Ostendorf, Laser direct writing of high refractive index polymer/TiO₂ nanocomposites, *Proc. SPIE* 8243 (2012) 824304.
- [15] Q. Guo, R. Ghadiri, T. Weigel, A. Aumann, E. L. Gurevich, C. Esen, O. Medenbach, W. Cheng, B. Chichkov, A. Ostendorf, Comparison of in situ and ex situ methods for synthesis of two-photon polymerization polymer nanocomposites, *Polymers* 6 (2014) 2037-2050.

- [16] M. Sangermano, L. Vescovo, N. Pepino, A. Chiolerio, P. Allia, P. Tiberto et al., M. Coisson, L. Suber, G. Marchegiani, Photoinitiator-Free UV-Cured Acrylic Coatings Containing Magnetite Nanoparticles, *Macromol. Chem. Phys.* 211 (2010) 2530–2535.
- [17] J. Wang, H. Xia, B. B. Xu, L. G. Niu, D. Wu, Q. D. Chen, H. B. Sun, Remote manipulation of micronanomachines containing magnetic nanoparticles, *Opt. Lett.* 34 (2009) 581-583.
- [18] H. Xia, J. Wand, Y. Tian, Q.-D. Chen, X.-B. Du, Y.-L. Zhang, Y. He, H.-B. Sun, Ferrofluids for Fabrication of Remotely Controllable Micro-Nanomachines by Two-Photon Polymerization, *Adv. Mater.*, 22 (29) (2010) 3204-3207.
- [19] Q. Guo, S. Xiao, A. Aumann, M. Jäger, M. Chakif, R. Ghadiri, C. Esen, M. Ma, A. Ostendorf, Using laser microfabrication to write conductive polymer/SWNTs nanocomposites, *J. Laser Micro/Nanoeng* 7 (2012) 44-48.
- [20] S. Ushiba, S. Shoji, K. Masui, P. Kuray, J. Kono, S. Kawata, 3D microfabrication of single-wall carbon nanotube/polymer composites by two-photon polymerization lithography, *Carbon* 59 (2013) 283-288.
- [21] A. J. G. Otuka, V. Tribuzi, M. R. Cardoso, G. F. B. de Almeida, A. R. Zanatta, D. S. Correa, C. R. Mendonca, Single-Walled Carbon Nanotubes Functionalized with Carboxylic Acid for Fabricating Polymeric Composite Microstructures, *J. Nanosci. Nanotechnol.* 15 (12) (2015) 9797-9801.
- [22] J.K.W. Sandler, J.E. Kirk, I.A. Kinloch, M.S.P. Shaffer, A.H. Windle, Ultra-low electrical percolation threshold in carbon-nanotube-epoxy Composites, *Polymer* 44 (2003) 5893–5899.

- [23] A. Moisala, Q. Li, I.A. Kinloch, A.H. Windle, Thermal and electrical conductivity of single- and multi-walled carbon nanotube-epoxy composites, *Comp. Sci. Tech.* 66 (2006) 1285–1288.
- [24] J. Z. Kovacs, B. S. Velagala, K. Schulte, W. Bauhofer, Two percolation thresholds in carbon nanotube epoxy composites, *Comp.Sci. Tech.* 67(2007) 922-928.
- [25] C. A. Martin, J. K. W. Sandler, M. S. P. Shaffer, M. K. Schwarz, W. Bauhofer, K. Schulte, A. H. Windle, Formation of percolating networks in multiwall carbon-nanotube-epoxy composites, *Comp. Sci. Tech.* 64 (2004) 2309-2316.
- [26] B. Kiss-Pataki, J. Tiusanen, G. Dobrik, Z. Vertesy, Z. E. Horvath, Visualization of the conductive paths in injection moulded MWNT/polycarbonate nanocomposites by conductive AFM, *Comp. Sci. Tech.* 90 (2014) 102-109.
- [27] Technical Datasheet Tuball™, OCSiAl LTD, accessed December, 6th, 2016, http://ocsial.com/assets/documents/TDS_TUBALL_4iN0GUh.pdf
- [28] Certificate of Analysis, Single walled nanotubes (SWNTs), accessed December, 6th, 2016, http://www.nanoamor.com/coa/coa_SWNT_1246YJS.pdf
- [29] B. Krause, R. Boldt, L. Häußler, P. Pötschke, Ultralow percolation threshold in polyamide 6.6/MWCNT composites, *Comp. Sci. Tech.* 114 (2015) 119–125.
- [30] B. Krause, P. Pötschke, E. Ilin, M. Predtechenskiy, Melt mixed SWCNT-polypropylene composites with very low electrical percolation, *Polymer* 98 (2016) 45-50.
- [31] T. Birr, U. Zywietz, P. Chhantyal, B. N. Chichkov, C. Reinhardt, Ultrafast surface plasmon-polariton logic gates and half-adder, *Opt. Exp.* 23 (25) (2015) 31755–31765.

[32] K. Obata, A. El-Tamer, L. Koch, U. Hinze, B.N. Chichkov, High-aspect 3D two-photon polymerization structuring with widened objective working range (WOW-2PP). *Light Sci. Appl.* 2 (2013) e116.

[33] P. Jyotishkumar, E. Logakis, S. M. George, J. Pionteck, L. Haussler, R. Haßler, P. Pissis, S. Thomas, Preparation and Properties of Multiwalled Carbon Nanotube/Epoxy-Amine Composites, *J. Appl. Polym. Sci.* 127 (2013) 3063-3073.